



Published in final edited form as:

*Differentiation*. 2016 December ; 92(5): 306–317. doi:10.1016/j.diff.2016.03.004.

## Mouse hypospadias: A critical examination and definition

Adriane Watkins Sinclair<sup>1</sup>, Mei Cao<sup>1</sup>, Joel Shen<sup>1</sup>, Paul Cooke<sup>2</sup>, Gail Risbridger<sup>3</sup>, Laurence Baskin<sup>1</sup>, and Gerald R. Cunha<sup>1,4</sup>

<sup>1</sup> Department of Urology, University of California San Francisco, 400 Parnassus Avenue, Box A610, San Francisco, CA 94143.

<sup>2</sup> Department of Physiological Sciences, University of Florida, Gainesville, Florida 32610.

<sup>3</sup> Monash Institute of Reproduction and Development, Monash University, Monash Medical Centre, Clayton, Victoria, Australia.

### Abstract

Hypospadias is a common malformation whose etiology is based upon perturbation of normal penile development. The mouse has been previously used as a model of hypospadias, despite an unacceptably wide range of definitions for this malformation. The current paper presents objective criteria and a definition of mouse hypospadias. Accordingly, diethylstilbestrol (DES) induced penile malformations were examined at 60 days postnatal (P60) in mice treated with DES over the age range of 12 days embryonic to 20 days postnatal (E12 to P20). DES-induced hypospadias involves malformation of the urethral meatus, which is most severe in DES E12-P10, DES P0-P10 and DES P5-P15 groups and less so or absent in the other treatment groups. A frenulum-like ventral tether between the penis and the prepuce was seen in the most severely affected DES-treated mice. Internal penile morphology was also altered in the DES E12-P10, DES P0-P10 and DES P5-P15 groups (with little effect in the other DES treatment groups). Thus, adverse effects of DES are a function of the period of DES treatment and most severe in the P0 to P10 period. In “estrogen mutant mice” (NERKI,  $\beta$ ERKO,  $\alpha$ ERKO and AROM+) hypospadias was only seen in AROM+ male mice having genetically-engineered elevation in serum estrogen. Significantly, mouse hypospadias was only seen distally at and near the urethral meatus where epithelial fusion events are known to take place and never in the penile midshaft, where urethral formation occurs via an entirely different morphogenetic process.

### Keywords

mouse; penis; penile urethra; hypospadias; estrogen

---

<sup>4</sup> Corresponding Author: Department of Urology, University of California San Francisco, 400 Parnassus Avenue, Box A610, San Francisco, CA 94143, Telephone: (650) 571-8070, gerald.cunha@ucsf.edu.

**Publisher's Disclaimer:** This is a PDF file of an unedited manuscript that has been accepted for publication. As a service to our customers we are providing this early version of the manuscript. The manuscript will undergo copyediting, typesetting, and review of the resulting proof before it is published in its final citable form. Please note that during the production process errors may be discovered which could affect the content, and all legal disclaimers that apply to the journal pertain.

## Introduction

In a previous paper the “window of susceptibility” of the developing mouse penis to the adverse developmental effects of diethylstilbestrol (DES) was analyzed at 10, 15 and 20 days postpartum in the following groups: (DES E12-E18, DES P0-P10, DES E12 to P10, DES P5 to P15 and DES P10 to P20) (Sinclair et al., 2016a). The rationale of this previous study was to examine the mouse penis shortly after the last DES injection to define the effects of DES during developmental periods. Penises of all 5 groups of DES-treated mice were reduced in size, and the most profound effects were seen in the DES E12-P10, DES P0-P10, and DES P5-P15 groups, thus defining a DES “programming window” for adverse effects centered in the early neonatal period. The most mild of effects on penile development were seen in the DES E12-E18 and DES P10-P20 groups. In the DES E12-P10 and DES P0-P10 groups adverse effects of DES on the MUMP cartilage and erectile bodies were observed shortly after the last DES injection persisted as enduring adult abnormalities. In contrast, in the DES P5-P15 group abnormalities in the MUMP cartilage and erectile bodies observed immediately after the last DES injection reverted to normality at 60 days postpartum. Thus, the induction of irreversible effects by DES also exhibited a “window of susceptibility” in the early neonatal period.

Expanding on our earlier study in which DES effects were examined in the neonatal period (P10 to P20) shortly after the DES treatment period, the current study follows cohorts of mice treated with DES developmentally (DES E12-E18, DES P0-P10, DES E12 to P10, DES P5 to P15 and DES P10 to P20) and analyzed in adulthood (60 days postnatal) to precisely define the resultant enduring DES-induced penile malformations by morphology and morphometric analysis. In so doing, a clearer understanding of estrogen-induced mouse hypospadias has been achieved.

Hypospadias is the second most common urogenital anomaly in boys occurring in approximately 1:200 to 1:300 male births (Baskin, 2000). The incidence of hypospadias in the USA has doubled in recent times (Paulozzi, 1999; Paulozzi et al., 1997). While the etiology of hypospadias in the majority of patients remains undefined, it is thought to involve both genetic susceptibility and environmental exposure to endocrine disruptors (Baskin and Ebbers, 2006; Kalfa et al., 2011; Willingham and Baskin, 2007; Skakkebaek et al., 2016; Wang and Baskin, 2008b). Surgery is the established treatment for hypospadias, and multiple surgeries are often required for a functionally acceptable reconstruction (Lee et al., 2013). In this regard, patients with severe hypospadias are at risk for surgical complications that may lead to life long difficulties with urination, sexual function and psychological problems. Thus, hypospadias is a significant medical condition that consumes substantial health care resources.

Hypospadias results from perturbation of normal penile development (Baskin et al., 1998), and can only be understood in the context of normal penile development. In humans, hypospadias consists of 3 related anomalies: (a) a urethral defect, (b) a preputial defect and (c) chordee (abnormal curvature of the penis). The abnormal urethral orifice in human hypospadias may be situated distally in the glans, at midshaft, or in the perineum (Cunha et

al., 2015). Associated with the defect in the urethral meatus is local absence or hypoplasia of the corpus spongiosum (Baskin et al., 1998).

Substantial differences in anatomy and development of the human versus the mouse penis invariably translate to profound differences in hypospadias in these two species (Cunha et al., 2015). While obvious abnormalities in the positioning of the urethral meatus are seen on physical examination in humans, the morphology of murine hypospadias is subtle. Midshaft malformations similar to human hypospadias have not been observed in mice treated perinatally with exogenous estrogens (Sinclair et al., 2016a; Blaschko et al., 2013; Mahawong et al., 2014b; a; Rodriguez et al., 2012) and may be due to the fact that mouse penile urethral development is substantially different from human penile development. Indeed, most of the murine penile urethra develops within the embryonic genital tubercle via canalization of the urethral plate to directly form most of the penile urethra, especially the midshaft region of the mouse urethra (Hynes and Fraher, 2004a; b; Seifert et al., 2008). In contrast, the mouse urethral meatus forms via an entirely different mechanism. The urethral plate of the mouse is not involved in formation of the urethral meatus since the urethral plate does not extend into the distal aspect of the genital tubercle (Sinclair et al., 2016a; Mahawong et al., 2014a; Schlomer et al., 2013). Instead, the mouse urethral meatus forms via fusion of the male urogenital mating protuberance (MUMP) with the MUMP ridge (Blaschko et al., 2013; Mahawong et al., 2014b; a; Rodriguez et al., 2011; Yang et al., 2010; Sinclair et al., 2016a). Consequently, estrogen-induced mouse hypospadias is an event restricted to the distal aspect of the urethra characterized by (a) altered patterning of elements constituting the urethral meatus, namely the male urogenital mating protuberance (MUMP) and MUMP ridge, (b) altered patterning of internal penile elements such as the os penis and urethral flaps relative to the urethral meatus and (c) absence or hypoplasia of the corpora cavernosa urethrae, the homologue of the human corpus spongiosum (Cunha et al., 2015). Whether such malformations seen in estrogen-treated mice are also relevant to mouse penile malformations elicited by other classes of agents (progestins, anti-androgens, phthalates) remains to be determined.

The current study describes the types of adult penile malformations induced developmentally by DES (hypospadias) in cohorts of mice treated with DES over the age range of E12 to P20, but examined in adulthood when enduring malformations are present.

## Materials and Methods

### Animals

Animal care and research protocols were approved by the Animal Care and Use Committee of the University of California, San Francisco (UCSF). Adult wild-type CD-1 and C57BL/6 mice (Charles River Breeding Laboratories, Wilmington, MA, USA) and their offspring were housed in polycarbonate cages ( $20 \times 25 \times 47 \text{ cm}^3$ ) with laboratory grade pellet bedding in the UCSF Pathogen Specific Barrier facility. Mice were given water *ad libitum* and fed LabDiet 5058 (PMI Nutrition International, P. O. Box 66812, St. Louis, MO 63166), whose content of phytoestrogen is incapable of eliciting vaginal cornification in ovariectomized adult mice (Buchanan et al., 1998). The following mutant mice were also used: estrogen receptor beta knockout ( $\beta$ ERKO) (Paul Cooke, University of Florida, Gainesville, FL),

estrogen receptor alpha knockout ( $\alpha$ ERKO) (Paul Cooke, University of Florida, Gainesville, FL), DNA binding mutation in estrogen receptor- $\alpha$  (NERKI) (Ellis Levin, University of California, Irvine, CA), and aromatase over-expresser (AROM+) (Gail Risbridger, Monash University, Melbourne, Australia). For all mutant mice, formalin fixed mouse rear ends containing the external genitalia were shipped to UCSG for processing. This study is based upon the analysis of 119 CD-1 and mutant mice.

### Hormonal Treatments

Pregnant CD-1 dams were weighed and injected subcutaneously on days 12, 14, 16, and 18 of gestation with DES at a concentration of 200ng/g body weight in ~5 $\mu$ l sesame oil vehicle. Control group dams were injected with 5 $\mu$ l sesame oil. Separate Hamilton syringes were used for sesame oil and DES. For postnatal DES treatment, the day of birth was counted as day 0, and pups were weighed and injected subcutaneously with either DES (200ng /gbw) or oil (5 $\mu$ l) on days 1, 3, 5, 7, 9 (DES P0-P10 & DES E12-P10), on days 5, 7, 9, 11, 13 (DES P5-P15) or on days 10, 12, 14, 16, 18 (DES P10-P20).

### Specimen Preparation and Analysis

DES- or oil-treated CD-1 mice were euthanized at the postnatal ages specified in Table 1. Sex was confirmed by gonadal inspection. External genitalia were dissected and fixed in 10% buffered formalin for a minimum of 24 hours. Seven micrometer thick sections were stained with hematoxylin and eosin as described previously (Sinclair et al., 2016a).

### Scanning electron microscopy

Surface details of adult mouse penises were elucidated using scanning electron microscopy (SEM) as described previously (Blaschko et al., 2013).

### Optical Projection tomography

Genital tubercles of mice at 16 days of gestation were fixed in 10% formalin, bleached with hydrogen peroxide, stained using a whole-mount immunofluorescence protocol (Abcam EP700Y anti-E-Cadherin monoclonal antibody, Alexa fluor 488 anti-rabbit secondary), optically cleared in benzyl alcohol and benzyl benzoate, embedded in agarose and imaged using a Biotronics OPT scanner 3001M as described (Li et al., 2014). Projected images from each channel were constructed into 3D voxel data sets with in-house software, which were then visualized using the Volocity software suite from PerkinElmer.

### Morphometric analysis

Metrics of pertinent key penile morphological features were obtained by counting the number of serial histologic sections from the distal tip of the adult penis to the beginning of the morphologic feature of interest as described previously (Schlomer et al., 2013) and illustrated in figure 5. Since several features are bilateral (e.g., urethral flaps and MUMP corpora cavernosa [MUMP CC]) and since perfect vertical orientation of the specimen in the paraffin block is not always possible, right and left features may appear in different closely associated sections. In this case, section numbers for the right and left elements were averaged to give the start point for each element pair.

## Corpora Cavernosa Urethrae Index

The corpora cavernosa urethrae (CCUr) are erectile bodies that begin bilaterally in the urethral flaps within the urethral lumen. As the erectile tissues continue proximally, the right and left erectile bodies become situated just ventral to the urethra. The CCUr, circumscribed by smooth muscle capsules, are closely associated with the urethra, and appear to be analogous to the corpus spongiosum in humans, which surrounds the urethra. Transverse sections were viewed, and the status of the CCUr was assessed via 3 criteria: (a) The CCUr as well-defined erectile bodies with distinct surrounding smooth muscle tunicas. (b) Red blood cells and/or blood vessel spaces observed within CCUr. (c) Urethral flaps present and fused ventrally with the urethra to form the erectile bodies. Each of these 3 observations was given a score of 0 points if the feature was completely absent, 0.5 if the trait was present but reduced or poorly developed, and 1 point for normal appearance. Therefore, for each penile specimen the CCUr index ranged from 0-3.

## Statistics

Comparison of morphological measures was done using either student's T tests, or ANOVA with Bonferroni correction. A p value < 0.05 was considered significant. A p value of 0.05 is represented by †, p 0.001 by #, and p 0.0001 by \*.

## Results

### Gross and histologic effects of perinatal DES on adult penile morphology

Scanning electron microscopy was performed on penises of 9 CD1 mice treated with oil or DES. Figure 1 depicts adult mouse penises in distal end-on, lateral and ventral views. As indicated previously (Rodriguez et al., 2011; Weiss et al., 2012; Yang et al., 2010; Phillips et al., 2015; Blaschko et al., 2013) the untreated or oil-treated adult mouse penis exhibits the following features: a distally bifid male urogenital mating protuberance (MUMP) (Rodriguez et al., 2011; Yang et al., 2010; Blaschko et al., 2013; Phillips et al., 2015). The MUMP is fused to the MUMP ridge and defines a Y-shaped urethral meatus (Blaschko et al., 2013; Rodriguez et al., 2011; Yang et al., 2010) (Fig. 1A). Peripheral to the MUMP ridge is a circumferential groove called the MUMP ridge groove (Fig. 1A). The ridge encircling the MUMP ridge groove is the internal prepuce (Blaschko et al., 2013) (Fig. 1A). The mouse glans penis is housed within the preputial space defined by the external prepuce (Phillips et al., 2015; Blaschko et al., 2013; Sinclair et al., 2016b) (Fig. 5B). Overall reduction in length of the glans penis was observed in all DES treatment groups (not illustrated), which corresponds to DES-induced reduction of penile length reported previously (Mahawong et al., 2014b; a; Sinclair et al., 2016a). Treatment with DES from E12 to E18 elicited mild truncation of the MUMP (Figs. 1H & N) with subtle distortion of the clefts within the MUMP ridge (Fig. 1B). Mice treated with DES from P0 to P10 and E12 to P10 exhibited profound distortion of external penile surface features. Both treatments elicited severe truncation of the MUMP, and the MUMP ridge was grossly malformed with a pattern of clefts and processes not seen in the oil-treated specimens (Figs. 1C, D, I, J, O, P). Accordingly, the normal Y-shaped urethral meatus was dramatically distorted. A constant feature of adult penises from the DES P0-P10 and DES E12-P10 (and an infrequent feature of DES P5-P15 mice) was a frenulum-like ventral tether that connected the ventral surface

of the penis to the inner surface of the external prepuce (Figs. 1 & 2). The thickness of the ventral tether, as well as other attachments of the penis to the inner surface of the external prepuce, were variable (Fig. 2). Mice treated with DES from P5-P15 exhibited mild truncation of the MUMP and minimal distortion of the MUMP ridge and urethral meatus (Figs. 1E, K, Q). Mice treated with DES from P10-P20 exhibited penile morphology similar to oil-treated specimens (Figs. 1F, L, R). SEM of AROM+,  $\alpha$ ERKO, and  $\beta$ ERKO has been reported previously (Blaschko et al., 2013). In summary, penises of  $\beta$ ERKO and  $\alpha$ ERKO mice exhibited minimal departure from the normal penile surface pattern. In contrast, penises of AROM+ mice exhibited severe truncation of the MUMP, profound distortion of the MUMP ridge and urethral meatus and ventral tethering (Fig. 2D) (Blaschko et al., 2013). Thus, in response to DES, increased severity of malformations of the penis corresponded to treatments that overlapped the period of P0 to P10. In addition, elevation of systemic estrogen levels associated with over-expression of aromatase in AROM+ mice (Li et al., 2001; Li et al., 2003) was associated with dramatic alterations of the distal aspect of the mouse penis (MUMP, MUMP ridge and urethral meatus) and ventral tethering (Blaschko et al., 2013).

### Effects of perinatal DES on the corpora cavernosa urethrae

The corpora cavernosa urethrae (CCUr) are erectile bodies located immediately ventral to the mouse urethra and which extend distally into the urethral flaps (Rodriguez et al., 2011) (Fig. 3A1 & 3A2). Figure 3 illustrates the normal morphology of the adult CCUr from a prenatally oil-treated mouse (Fig. 3A1 & 3A2). Abnormal CCUr morphology was observed in mice of the DES E12-P10 and DES P0-P10 groups (Fig. 3B1, 3B2, 3C1, 3C2) and in adult AROM+ mice (Figs. 3D1 and 3D2). Epifluorescence of H&E stained sections illuminated by the Cy3 HYQ filter combination is particularly effective in visualizing the smooth muscle capsules that normally encompass the CCUr (Figs 3A2, 3B2 3C2 & 3D2). The morphology of the CCUr of all other treatment groups was normal or near normal (Oil, DES P5-P15 and DES P10-P20) (not illustrated). In oil-treated mice well-defined CCUr surrounded by smooth muscle capsules were evident that contained considerable numbers of red blood cells (Figs. 3A1 & 3A2). In contrast, in the DES E12-P10 and DES P0-P10 specimens (Figs. 3B1, 3B2, 3C1, 3C2) the CCUr were indistinct, lacked smooth muscle capsules, and red blood cells were not apparent. In adult AROM+ mice, the CCUr are evident, but not well demarcated (Figs. 3D1 and 3D2). The CCUr were normal in all other mutants examined (NERKI,  $\beta$ ERKO,  $\alpha$ ERKO). Urethral flaps are not present in the sections depicted in figure 3, but were evaluated in more distal sections.

A corpora cavernosa urethrae index (as described in the Materials and Methods) was used to quantify the magnitude of effect of DES on this parameter. The CCUr index score for DES-treated mice was dependent upon the timing of DES treatment (Fig. 4). Mice treated from with DES from E12 to E18 as well as from P10 to P20 exhibited an adult CCUr index statistically similar to that of the oil-treated mice with values between 2.5 and 3. In contrast, mice treated with DES from P0 to P10, E12 to P10 and P5 to P15 exhibited a statistically significant reduction in the adult CCUr index value. Indeed, in the DES E12-P10 group the CCUr index value was zero (Fig. 4). The CCUr index of NERKI,  $\alpha$ ERKO, and  $\beta$ ERKO

mice was indistinguishable from that of oil-treated CD-1 and C57BL/6 mice (~2.3 to 2.8), while the CCUr index of AROM+ mice was significantly reduced to ~1.4 (Fig. 4).

### Morphometric effects of perinatal DES on the adult mouse penis

Estrogens such as DES as well as germline mutations that affect estrogen signaling have been shown to alter the pattern of external and internal penile features (Blaschko et al., 2013; Mahawong et al., 2014b; a; Sinclair et al., 2016a; Rodriguez et al., 2012) (Fig. 1). To better appreciate the types and extent of such malformations, morphometric analysis of penile structures was carried out in mice treated with DES during a variety of developmental periods. Figure 5 indicates the types of measures and how they were made. Absolute MUMP length (tip of the MUMP to distal aspect of the MUMP ridge) was significantly reduced in all DES treatment groups with the exception of the DES P10-P20 group whose MUMP was reduced somewhat, but not significantly (Figs. 6A). In all mutant mice, absolute MUMP length was also significantly reduced relative to CD-1 mice (Fig. 6D). This comparison is questionable as all mutant mice used in this study are on the C57Bl/6 background. When MUMP length was compared to MUMP length of C57Bl/6 mice, significant reduction in MUMP length was only seen in AROM+ mice with genetically engineered elevation of systemic estrogen (Figs. 6D). To determine if reduction in MUMP length was simply a function of overall reduction in penile length, we normalized MUMP length in DES-treated and mutant mice by two surrogates of penile length, namely (a) penile tip to distal tip of the os penis and (b) penile tip to the proximal terminus of the internal preputial space as described in figure 5. For the DES treatment groups the magnitude of CD-1 MUMP length reduction was attenuated somewhat when normalized to penile length (Bone Depth), but was statistically significant for all DES treatment groups except the DES P10-P20 group whose MUMP was reduced, but not significantly (Fig. 6B). Similar reductions in CD-1 MUMP length were obtained when normalized to the proximal terminus of the internal preputial space (Fig. 6C). Thus, reduction of MUMP length is partly a function of the overall reduction in penile length, more importantly is a function of the period of DES treatment.

When MUMP length of the mutant mice was normalized to surrogates of penile length (penile tip to distal tip of the os penis (Fig. 6E) or penile tip to proximal terminus of the internal preputial space (Fig. 6F) significant reduction in MUMP length was only seen in AROM+ mice.

The mouse has two prepuces, an external and an internal prepuce. The external prepuce forms the prominent elevation in the perineum and creates the voluminous preputial space housing the penis (Sinclair et al., 2016a). The external prepuce is not homologous to the human prepuce, which is integral to the penis, while the internal mouse prepuce is homologous to the human prepuce and has a ventral cleft (Blaschko et al., 2013; Cunha et al., 2015). Accordingly, we measured absolute length of the ventral cleft in the internal prepuce (distal aspect of internal prepuce to proximal end of cleft in internal prepuce). In DES-treated CD-1 mice absolute length of the internal preputial cleft was not affected statistically irrespective of the treatment periods (Fig. 7A). However, when normalized to surrogates of penile size, length of the internal preputial cleft was increased statistically in the DES E12-E18, DES P0-P10 and DES E12-P10 groups (Fig. 7B & C). In the mutant mice

length of the internal preputial cleft was significantly increased only in AROM+ mice when normalized to a surrogate of penile length (Fig. 7F).

The distance from the distal penile tip to the distal tips of the urethral flaps (urethral flap depth) was profoundly affected by DES treatment, and the effect was the same whether judged as an absolute measurement or normalized to penile length (Fig. 8A-C). For the DES P0-P10 and DES E12-P10 groups, the urethral flaps were entirely absent and thus a score of zero was recorded. For the DES P5-P15 groups the distance from the distal penile tip to the distal tips of the urethral flaps was also reduced significantly (Fig. 8A-C). For the mutant mice, the absolute distance from the distal penile tip to the distal tips of the urethral flaps was significantly reduced in AROM+ mice when compared to CD-1, but was significantly increased when compared with C57Bl/6 mice (Fig. 8D). When normalized to surrogates of penile length distance from the distal penile tip to the distal tips of the urethral flaps was significantly increased in AROM+ and  $\alpha$ ERKO mice (Fig. 8E-F).

Perinatal DES also affected the depth of the internal preputial space. Absolute depth of the internal preputial space was significantly decreased in the DES P0-P10 and DES E12-P10 groups (Fig. 9A). However, depth of the internal preputial space was increased in several DES treatment groups (DES E12-E18, DES P0-P10, DES E12-P10 and DES P5-P15) when the data were normalized to overall penile length based upon bone depth (Fig. 9B) due to the overall global reduction in length of the glans penis of the mouse. For all mutant mice absolute depth of the internal preputial space was not significantly altered (Fig. 9C), but when normalized to bone depth or depth of the internal preputial space was significantly increased in AROM+ mice (Fig. 9D).

### Status of the urethral plate at 16 days of gestation

In our recent papers (Cunha et al., 2015; Sinclair et al., 2016a) we have announced the idea that development of the mouse penile urethra occurs in two phases through vastly different mechanisms. Most of the mouse penile urethra forms by direct canalization of the urethral plate during embryonic periods (Hynes and Fraher, 2004b; Seifert et al., 2008). However, subsequently during the neonatal period the distal aspect of the urethra and especially the urethral meatus forms via a series of fusion events (Blaschko et al., 2013; Sinclair et al., 2016a; Cunha et al., 2015). The critical observation in support of this duality of developmental mechanism concerns the proximal-distal extent of the urethral plate within the genital tubercle, that is, whether the urethral plate extends all the way to the distal aspect of the developing genital tubercle or not. To elucidate this issue, we carried out OPT on genital tubercles at 16 days of gestation (Fig. 10). Figure 10A is a surface rendering of the day E16 genital tubercle. Transverse OPT sections 10a-h are shown, and the positions of the transverse sections are indicated on the OPT wholemount images (Fig. 10A-C). The tubular urethra and the urethral plate extend only to the approximate position of section 10e. The solid urethral plate does not exist in sections (Fig. 10a-d) and instead a ventral groove is present, which we have reported previously in the mouse genital tubercle at birth (Mahawong et al., 2014a; Sinclair et al., 2016a).



## Discussion

Human hypospadias is a congenital malformation of penile development that involves an abnormal urethral meatus, a ventral defect in the prepuce and chordee (curvature of the penis). The abnormal urethral meatus may be located distally in the glans, at midshaft or in the perineum. Associated with the abnormal urethral meatus is a deficiency in the corpus spongiosum, which normally provides bulk to the urethral wall. Thus, in human hypospadias the anatomical defects consists of an absence of the ventral wall of the urethra, a deficiency in the corpus spongiosum, a deficiency in human penile skin at the site of the abnormal urethral meatus and distally and a deficiency in the prepuce (Cunha et al., 2015; Sinclair et al., 2016a). Estrogenic endocrine disruptors have been suggested as a potential cause of human hypospadias (Vilela et al., 2007; Wang and Baskin, 2008a). Indeed, the incidence of human hypospadias is elevated in DES sons, who were exposed in utero to this potent estrogen (Klip et al., 2002; Jouannic and Benifla, 2005; Palmer et al., 2005; Pons et al., 2005). Of course, the cause of hypospadias is multifactorial and may involve a spectrum of hormonal agents (estrogens, anti-androgens, progestins) as well as genetic alterations (Cunha et al., 2015).

In mice treated perinatally with DES and other estrogens we have never observed midshaft or perineal urethral malformations based upon the analysis of 239 mice in 5 separate papers (Kim et al., 2004; Mahawong et al., 2014b; a; Blaschko et al., 2013; Sinclair et al., 2016a), which may mean that midshaft, proximal shaft or scrotal perineal urethral malformations are not possible in mice. Perinatally DES-treated and AROM+ mice (having elevated serum estradiol) exhibited malformations of the distal aspect of the penis that included severe truncation of the MUMP as well as malformation of the MUMP ridge that forms the urethral meatus. Other mutant mice examined ( $\alpha$ ERKO,  $\beta$ ERKO and NERKI) exhibited a normal urethral meatus (Blaschko et al., 2013). Accordingly, the common feature for an abnormal urethral meatus is elevated estrogen.

The striking morphological differences between human hypospadias and the penile malformations seen in perinatally estrogen-treated mice is due to substantial differences in the morphogenesis of the penile urethra in these two species. In humans, a solid urethral epithelial plate forms on the ventral aspect of the genital tubercle (embryonic phallus) that extends from the perineum to the distal aspect of the genital tubercle. The urethral plate subsequently canalizes via an “opening zipper” to form a broadly open urethral groove. The edges of the urethral groove (urethral folds) then approach each other and fuse in the midline (“closing zipper”) to form the human penile urethra. This fusion process begins proximally and extends distally to complete urethral development to its terminus in the glans (Li et al., 2014). Human hypospadias presumably occurs as a result of (a) failure of formation of the urethral plate, (b) failure of urethral plate canalization, or (c) failure of fusion of the urethral folds.

In mice the mechanism of penile urethral development appears to occur via two very different morphogenetic mechanisms (Cunha et al., 2015; Hynes and Fraher, 2004b; Seifert et al., 2008). As in humans a solid urethral plate forms in mice which extends distally, but not all of the way to the distal terminus of the genital tubercle as seen in figure 12

(Mahawong et al., 2014a) and in figure 10 of the current paper. Most of the mouse penile urethra forms by direct canalization of the embryonic urethral plate and detachment of the urethral plate from the overlying epidermis, a process that occurs prenatally in mice (Seifert et al., 2008; Hynes and Fraher, 2004b). This mechanism cannot account for formation of the distal aspect of the penile urethra (and especially the urethral meatus) because at 16 days of gestation (Fig. 10), birth and thereafter the murine urethral plate is not present in the distal aspect of the genital tubercle as reported previously (Sinclair et al., 2016a; Mahawong et al., 2014a). Instead at 16 days of gestation and at birth a ventral groove is present on the distal aspect of the mouse genital tubercle whose edges fuse in the midline to form the distal aspect of the mouse penile urethra and the urethral meatus (Mahawong et al., 2014a; Sinclair et al., 2016a).

Several lines of evidence support the notion that the mouse urethral meatus forms via fusion of the MUMP and MUMP ridge (Blaschko et al., 2013; Mahawong et al., 2014b; a; Rodriguez et al., 2011; Yang et al., 2010; Schlomer et al., 2013). The normal adult MUMP ridge (forming most of the urethral meatus) has a series of characteristic clefts that we believe are manifestations of developmental fusion events seen in untreated, oil-treated,  $\alpha$ ERKO,  $\beta$ ERKO and NERKI mice (Blaschko et al., 2013). The pattern of processes and clefts in the MUMP ridge are profoundly abnormal in DES E12-P10, DES P0-P10, DES P5-P15 and AROM+ mice, suggesting an estrogenic etiology to these malformations. Given the importance of fusion events in formation of the human urethra and formation of the urethral meatus in mice, it is likely that common molecular mechanisms may be involved in both species in these areas.

The penile malformations induced perinatally in mice with DES merit the descriptor, hypospadias for several reasons: (a) Perinatally DES-treated adult mice exhibit an abnormal urethral meatus (Blaschko et al., 2013; Mahawong et al., 2014b; a; Sinclair et al., 2016a). (b) The corpora cavernosa urethrae (homologues of the human corpus spongiosum) are hypoplastic and exhibit a dramatic reduction in the corpora cavernosa urethrae index (Mahawong et al., 2014a; Sinclair et al., 2016a; Cunha et al., 2015). (c) The external and internal prepuces are malformed (Mahawong et al., 2014b; a). (d) Ventral tethering of the penis to the inner surface of the external prepuce is diagnostic of an abnormality of penile skin (Blaschko et al., 2013; Mahawong et al., 2014a; Sinclair et al., 2016a). All of these features of mouse hypospadias have counterparts in human hypospadias (Cunha et al., 2015; Sinclair et al., 2016a) and are indicative of a global disturbance in the patterning of external and internal penile features in regions of the mouse penis whose development involves fusion events similar in a general sense to those occurring in human penile development.

One of the striking differences between mouse and human external genitalia is that the mouse has 2 prepuces and the human has 1 prepuce (Blaschko et al., 2013; Sinclair et al., 2016b). The mouse external prepuce forms a voluminous space housing the penis and forms the prominent perineal appendage (Sinclair et al., 2016b). The mouse internal prepuce is homologous to the human foreskin since in both species these skin flaps are integral to the penis (Blaschko et al., 2013; Sinclair et al., 2016b). In the course of mouse penile development, the penile stroma is surrounded by the external preputial lamina which has a ventral gap through which penile stroma is continuous with preputial stroma (Mahawong et

al., 2014b; a; Sinclair et al., 2016a). During normal delamination of the external preputial lamina (which occurs over an extended period and is completed at ~30 days postnatal) the continuity of stroma between the penis and the external prepuce is obliterated resulting in a penis freely mobile (untethered) within the preputial space (Blaschko et al., 2013; Mahawong et al., 2014a; Sinclair et al., 2016a; Mahawong et al., 2014b). Indeed, normally the penile surface epithelium is continuous with inner preputial epithelium only proximally where penile surface epithelium reflects onto the inner preputial epithelium in the depth of the preputial space. However, in DES P0-P10, DES E12-P10, AROM+, and some DES P5-P15 mice, the continuity of penile and preputial stroma is maintained along the shaft of the penis as a frenulum-like connection between the ventral aspect of the penis and the inner preputial wall, signifying an abnormality in ventral penile skin (Blaschko et al., 2013; Mahawong et al., 2014a; Sinclair et al., 2016a). The consistent finding of ventral tethering of the penis in AROM+ mice indicates that physiological elevation in endogenous estradiol is sufficient to elicit this malformation. At 4 months postnatal AROM+ male mice have dramatically elevated serum estradiol levels (98-225pg/ml), whereas in wild-type male mice serum estradiol is below the detection level (Li et al., 2001). Thus, estrogen-induced ventral tethering of the penis is not unique to synthetic estrogens such as DES, but appears to be a general aspect of elevated estrogen. The ventral tether frequently extends distally to the urethral meatus and completely or partially abrogates the ventral cleft in the MUMP ridge and the ventral cleft in the internal prepuce thus distorting the urethral meatus (Fig. 1).

The ventral tether seen consistently in perinatally DES-treated male mice (DES P0-P10, DES E12-P10 and to a lesser extent in DES P5-P15) poses severe problems for these mice. Initially such DES-treated mice have a persistently wet urine-stained perineum. Subsequently, retention of urine in the preputial space results in subsequent crystallization of preputial stones (Mahawong et al., 2014a), which can become large hard foreign bodies causing erosion of the distal aspect of the penis (Warner et al., 1979). This suggests that urination in mice normally involves extension of the penis beyond the preputial meatus so that urine can be expelled cleanly beyond the prepuce. The presence of a ventral tether appears to restrict penile mobility and impair projection of the penis beyond the preputial meatus during urination and presumably also during mating.

One striking feature of human hypospadias is hypoplasia of the corpus spongiosum in and around the abnormal urethral meatus. In similar fashion, DES elicits abnormality of the corpora cavernosa urethrae, the mouse homologue of the human corpus spongiosum (Mahawong et al., 2014a; Sinclair et al., 2016a; Cunha et al., 2015). As in humans, hypoplasia of the corpora cavernosa urethrae is an event that is restricted to the distal aspect of the mouse glans penis that is easily recognized in histological sections and manifested as a substantial reduction in the corpora cavernosa urethrae index (Fig. 4). Malformation of the urethral flaps (the distal extension of the corpora cavernosa urethrae) as well as the corpora cavernosa urethrae themselves is most severe when the timing of DES exposure overlaps into the P0 to P10 time period, thus reinforcing the “window of susceptibility” to DES reported earlier (Sinclair et al., 2016a). One aspect of DES-induced malformation of the corpora cavernosa urethrae is the absence of well-defined smooth muscle capsules surrounding the vascular spaces. Goyal has demonstrated estrogen-induced impairment of smooth muscle differentiation in penises of rats treated neonatally with DES, an effect

mitigated by co-administration of the ICI anti-estrogen (Goyal et al., 2005; Okumu et al., 2012).

A key point regarding mouse hypospadias is that it is important to diagnose it in adulthood as some of the estrogen-induced (and finasteride-induced) malformations seen developmentally represent retardations in development which resolve to normality after discontinuation of drug treatment (Sinclair et al., 2016a; Kim et al., 2004; Iguchi et al., 1991). When penile malformations are observed late in gestation in hormonally-treated or mutant mice, the tacit (but unproven) assumption is that embryonic genital tubercle malformations are irreversible and will progress to enduring adult penile malformations. Without allowing embryonic penile malformations to progress to adulthood (as is the case for many papers), it is impossible to know whether embryonic genital tubercle defects are indicative of enduring adult malformations or are merely reversible developmental retardations. Obviously, enduring adult malformations elicited by perinatal DES treatment have developmental counterparts, which require detailed analysis to know which neonatal penile malformations endure into adulthood and which resolve to normality following discontinuation of DES treatment (Sinclair et al., 2016a). Enduring adult penile malformations are obvious and easily identified, and thus analysis in adulthood is highly recommended.

Morphometric analysis confirms that DES affects the patterning of internal and external features in the mouse penis, increasing or decreasing certain morphometric measures. Whether a penile element is increased or decreased in size is dependent upon the timing of DES treatment, whether the data are expressed as absolute distance or normalized to a surrogate of penile length, and perhaps also on differential sensitivity of an element to exogenous estrogen. MUMP length (Fig. 6) and distal MUMP tip to urethral flaps length (Fig. 8) were reduced in several DES-treated groups absolutely and also when normalized to penile length. Length of the internal preputial cleft (Fig. 7) showed no effect when expressed as absolute length, but showed significant increases in the DES E12-E18, DES P0-P10 and DES E12-P10 groups when the data was normalized to overall reduction in penile length. A similar trend was seen in the AROM+ mouse. In the case of depth of the internal preputial space (Fig. 9) this parameter exhibited absolute reduction in length, but when normalized to surrogates of penile length this parameter was increased. This means that these two measures (penile length and depth of the internal preputial space) are differentially affected by perinatal DES treatment. Taken together our morphometric studies emphasize the idea that DES as well as elevated serum estrogen (AROM+) affects the overall patterning of external and internal penile elements. In some cases the reduction in an individual element occurs in concert with overall DES-induced reduction in penile length. In other cases, the change in the value of an individual element may be greater or lesser proportionally than the overall reduction in penile length noted developmentally in pre- and neonatally DES-treated mice at 5 days postnatal (Mahawong et al., 2014b; a; Sinclair et al., 2016a) as well as in adulthood (60-days postnatal, this paper). Reductions in overall penile length as well as other measures may be due to DES-induced reduction in proliferative activity or apoptosis, although neither of these possibilities was examined in the current paper. Many effects seen in response to synthetic (DES) were also seen in AROM+ mice in which natural estrogens

(estradiol) are elevated. Whether this is true for other types of agents (anti-androgens, progestins, phthalates, etc) remains to be determined.

In conclusion, hypospadias in humans and mice is substantially different owing to differences in the developmental mechanisms of formation of the penile urethra. The generally accepted morphogenesis of hypospadias in humans is solidly based upon failure of fusion of the urethral folds to convert the urethral groove into the penile urethra. In the case of the mouse fusion events (similar to those in the developing human penis) are observed only in the distal aspect of the penile urethra and especially manifest in the formation of the urethral meatus. It is these distal estrogen-induced penile malformations in the mouse that constitute mouse hypospadias. It remains to be determined whether other hormonally active agents elicit similar penile malformations in the mouse penis. Given the many chemicals in the environment having estrogenic properties (McLachlan, 1981), an important (but unresolved) question is whether the burden of environmental estrogens are a factor in human hypospadias. Dose-response studies over a broad concentration range in mice may shed light on this question.

## Acknowledgments

This work was supported by NIH grant RO1 DK0581050.

## Abbreviations

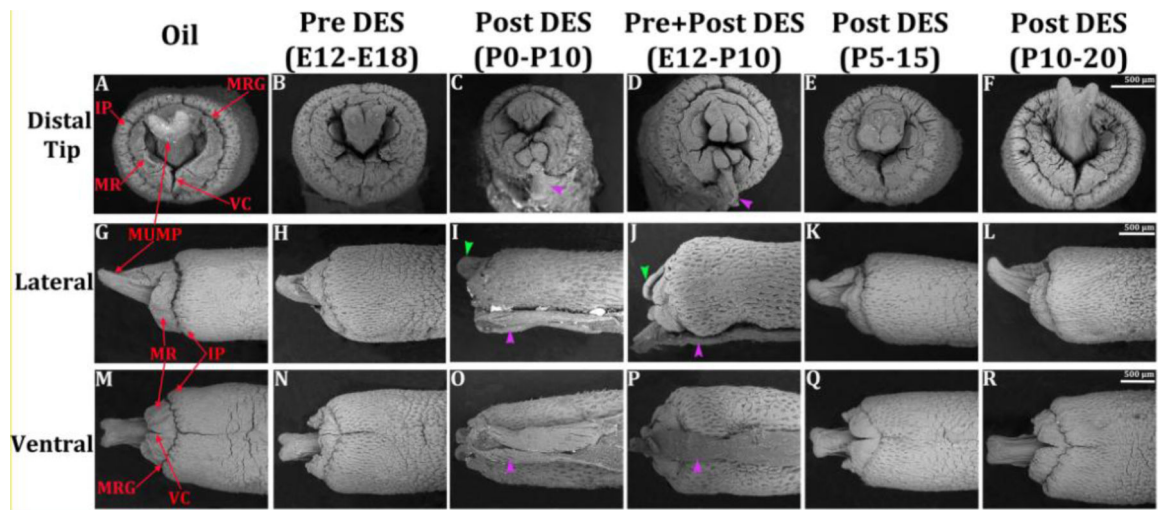
<b>DES</b>	Diethylstilbestrol
<b>E</b>	embryonic
<b>P</b>	postnatal
<b>OPT</b>	optical projection tomography
<b>MUMP</b>	male urogenital mating protuberance

## References

- Baskin LS. Hypospadias and urethral development. *The Journal of urology*. 2000; 163:951–956. [PubMed: 10688029]
- Baskin LS, Ebbers MB. Hypospadias: anatomy, etiology, and technique. *J Pediatr Surg*. 2006; 41:463–472. [PubMed: 16516617]
- Baskin LS, Erol A, Li YW, Cunha GR. Anatomical studies of hypospadias. *The Journal of urology*. 1998; 160:1108–1115. [PubMed: 9719287]
- Blaschko SD, Mahawong P, Ferretti M, Cunha TJ, Sinclair A, Wang H, Schlomer BJ, Risbridger G, Baskin LS, Cunha GR. Analysis of the effect of estrogen/androgen perturbation on penile development in transgenic and diethylstilbestrol-treated mice. *Anatomical record*. 2013; 296:1127–1141.
- Buchanan DL, Kurita T, Taylor JA, Lubahn DL, Cunha GR, Cooke PS. Role of stromal and epithelial estrogen receptors in vaginal epithelial proliferation, stratification and cornification. *Endocrinology*. 1998; 139:4345–4352. [PubMed: 9751518]
- Cunha GR, Sinclair A, Risbridger G, Hutson J, Baskin LS. Current understanding of hypospadias: relevance of animal models. *Nature reviews. Urology*. 2015; 12:271–280. [PubMed: 25850792]

- Goyal HO, Braden TD, Williams CS, Dalvi P, Mansour M, Williams JW. Estrogen-induced abnormal accumulation of fat cells in the rat penis and associated loss of fertility depends upon estrogen exposure during critical period of penile development. *Toxicological sciences : an official journal of the Society of Toxicology*. 2005; 87:242–254. [PubMed: 15976194]
- Hynes PJ, Fraher JP. The development of the male genitourinary system: II. The origin and formation of the urethral plate. *Br J Plast Surg*. 2004a; 57:112–121. [PubMed: 15037165]
- Hynes PJ, Fraher JP. The development of the male genitourinary system: III. The formation of the spongiose and glandular urethra. *Br J Plast Surg*. 2004b; 57:203–214. [PubMed: 15006521]
- Iguchi T, Uesugi Y, Takasugi N, Petrow V. Quantitative analysis of the development of genital organs from the urogenital sinus of the fetal male mouse treated prenatally with a 5 alpha-reductase inhibitor. *J Endocrinol*. 1991; 128:395–401. [PubMed: 2013746]
- Jouannic JM, Benifla JL. Hypospadias in sons of women exposed to diethylstilbestrol: a true trans-generational effect? *Prenatal diagnosis*. 2005; 25:1071–1072. [PubMed: 16302166]
- Kalfa N, Philibert P, Baskin LS, Sultan C. Hypospadias: interactions between environment and genetics. *Molecular and cellular endocrinology*. 2011; 335:89–95. [PubMed: 21256920]
- Kim KS, Torres CR Jr, Yucel S, Raimondo K, Cunha GR, Baskin LS. Induction of hypospadias in a murine model by maternal exposure to synthetic estrogens. *Environ Res*. 2004; 94:267–275. [PubMed: 15016594]
- Klip H, Verloop J, van Gool JD, Koster ME, Burger CW, van Leeuwen FE, Group OP. Hypospadias in sons of women exposed to diethylstilbestrol in utero: a cohort study. *Lancet*. 2002; 359:1102–1107. [PubMed: 11943257]
- Lee OT, Durbin-Johnson B, Kurzrock EA. Predictors of secondary surgery after hypospadias repair: a population based analysis of 5,000 patients. *The Journal of urology*. 2013; 190:251–255. [PubMed: 23376710]
- Li X, Makela S, Streng T, Santti R, Poutanen M. Phenotype characteristics of transgenic male mice expressing human aromatase under ubiquitin C promoter. *The Journal of steroid biochemistry and molecular biology*. 2003; 86:469–476. [PubMed: 14623546]
- Li X, Nokkala E, Yan W, Streng T, Saarinen N, Warri A, Huhtaniemi I, Santti R, Makela S, Poutanen M. Altered structure and function of reproductive organs in transgenic male mice overexpressing human aromatase. *Endocrinology*. 2001; 142:2435–2442. [PubMed: 11356692]
- Li Y, Sinclair A, Cao M, Shen J, Choudhry S, Cunha GR, Baskin L. Canalization of the urethral plate precedes fusion of the urethral folds during male penile urethral development: the double zipper hypothesis. *J. Urology*. 2014; 193:1353–1359.
- Mahawong P, Sinclair A, Li Y, Schlomer B, Rodriguez E, Ferretti M, Liu B, Baskin LS, Cunha GR. Comparative effects of neonatal diethylstilbestrol on external genitalia development in adult males of two mouse strains with differential estrogen sensitivity. *Differentiation; research in biological diversity*. 2014a; 88:70–83. [PubMed: 25449353]
- Mahawong P, Sinclair A, Li Y, Schlomer B, Rodriguez E, Ferretti M, Liu B, Baskin LS, Cunha GR. Prenatal diethylstilbestrol induces malformation of the external genitalia of male and female mice and persistent second-generation developmental abnormalities of the external genitalia in two mouse strains. *Differentiation; research in biological diversity*. 2014b; 88:51–69. [PubMed: 25449352]
- McLachlan, JA. *Estrogens in the Environment*. Elsevier/North Holland; New York: 1981.
- Okumu LA, Bruinton S, Braden TD, Simon L, Goyal HO. Estrogen-induced maldevelopment of the penis involves down-regulation of myosin heavy chain 11 (MYH11) expression, a biomarker for smooth muscle cell differentiation. *Biology of reproduction*. 2012; 87:109. [PubMed: 22976277]
- Palmer JR, Wise LA, Robboy SJ, Titus-Ernstoff L, Noller KL, Herbst AL, Troisi R, Hoover RN. Hypospadias in sons of women exposed to diethylstilbestrol in utero. *Epidemiology*. 2005; 16:583–586. [PubMed: 15951681]
- Paulozzi LJ. International trends in rates of hypospadias and cryptorchidism. *Environmental health perspectives*. 1999; 107:297–302. [PubMed: 10090709]
- Paulozzi LJ, Erickson JD, Jackson RJ. Hypospadias trends in two US surveillance systems. *Pediatrics*. 1997; 100:831–834. [PubMed: 9346983]

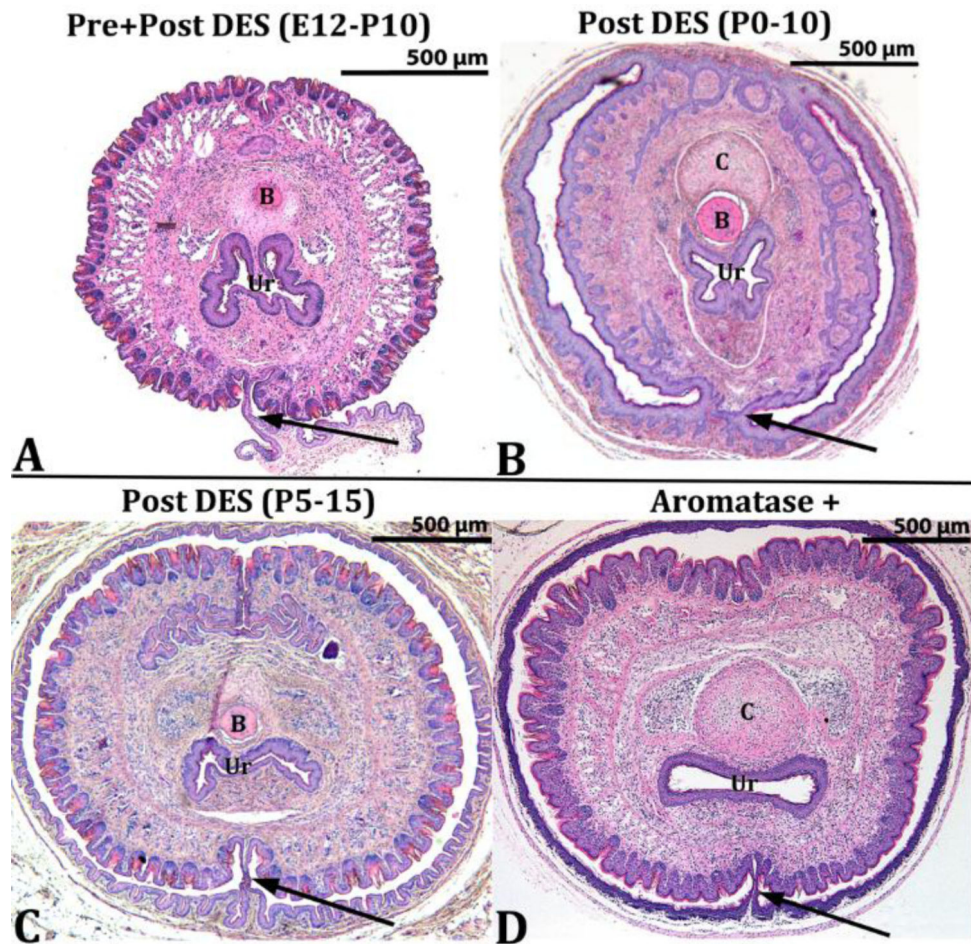
- Phillips TR, Wright DK, Gradie PE, Johnston LA, Pask AJ. A Comprehensive Atlas of the Adult Mouse Penis. Sexual development : genetics, molecular biology, evolution, endocrinology, embryology, and pathology of sex determination and differentiation. 2015; 9:162–172.
- Pons JC, Papiernik E, Billon A, Hessabi M, Duyme M. Hypospadias in sons of women exposed to diethylstilbestrol in utero. Prenatal diagnosis. 2005; 25:418–419. [PubMed: 15906411]
- Rodriguez E Jr, Weiss DA, Ferretti M, Wang H, Menshenina J, Risbridger G, Handelsman D, Cunha G, Baskin L. Specific morphogenetic events in mouse external genitalia sex differentiation are responsive/dependent upon androgens and/or estrogens. Differentiation; research in biological diversity. 2012; 84:269–279. [PubMed: 22925506]
- Rodriguez E Jr, Weiss DA, Yang JH, Menshenina J, Ferretti M, Cunha TJ, Barcellos D, Chan LY, Risbridger G, Cunha GR, Baskin LS. New insights on the morphology of adult mouse penis. Biology of reproduction. 2011; 85:1216–1221. [PubMed: 21918128]
- Schlomer BJ, Feretti M, Rodriguez E Jr, Blaschko S, Cunha G, Baskin L. Sexual differentiation in the male and female mouse from days 0 to 21: a detailed and novel morphometric description. The Journal of urology. 2013; 190:1610–1617. [PubMed: 23473905]
- Seifert AW, Harfe BD, Cohn MJ. Cell lineage analysis demonstrates an endodermal origin of the distal urethra and perineum. Developmental biology. 2008; 318:143–152. [PubMed: 18439576]
- Sinclair AW, Cao M, Baskin L, Cunha GR. Diethylstilbestrol-Induced Mouse Hypospadias: “Window of Susceptibility”. Differentiation; research in biological diversity. 2016a; 91:1–18.
- Sinclair AW, Glickman SE, Baskin L, Cunha GR. Anatomy of mole external genitalia: Setting the record straight. Anatomical record. 2016b; 299:385–399.
- Skakkebaek NE, Rajpert-De Meyts E, Buck Louis GM, Toppari J, Andersson AM, Eisenberg ML, Jensen TK, Jorgensen N, Swan SH, Sapra KJ, Ziebe S, Priskorn L, Juul A. Male Reproductive Disorders and Fertility Trends: Influences of Environment and Genetic Susceptibility. Physiological reviews. 2016; 96:55–97. [PubMed: 26582516]
- Vilela ML, Willingham E, Buckley J, Liu BC, Agras K, Shiroyanagi Y, Baskin LS. Endocrine disruptors and hypospadias: role of genistein and the fungicide vinclozolin. Urology. 2007; 70:618–621. [PubMed: 17905137]
- Wang MH, Baskin LS. Endocrine Disruptors, Genital Development and Hypospadias. J Androl. 2008a
- Wang MH, Baskin LS. Endocrine disruptors, genital development, and hypospadias. Journal of andrology. 2008b; 29:499–505. [PubMed: 18497336]
- Warner MR, Warner RL, Clinton CW. Reproductive tract calculi, their induction, age incidence, composition and biological effects in Balb/c crgl mice injected as newborns with estradiol-17 $\beta$ . Biol. Reprod. 1979; 20:310–322. [PubMed: 36930]
- Weiss DA, Rodriguez E Jr, Cunha T, Menshenina J, Barcellos D, Chan LY, Risbridger G, Baskin L, Cunha G. Morphology of the external genitalia of the adult male and female mice as an endpoint of sex differentiation. Molecular and cellular endocrinology. 2012; 354:94–102. [PubMed: 21893161]
- Willingham E, Baskin LS. Candidate genes and their response to environmental agents in the etiology of hypospadias. Nat Clin Pract Urol. 2007; 4:270–279. [PubMed: 17483812]
- Yang JH, Menshenina J, Cunha GR, Place N, Baskin LS. Morphology of mouse external genitalia: implications for a role of estrogen in sexual dimorphism of the mouse genital tubercle. The Journal of urology. 2010; 184:1604–1609. [PubMed: 20728117]



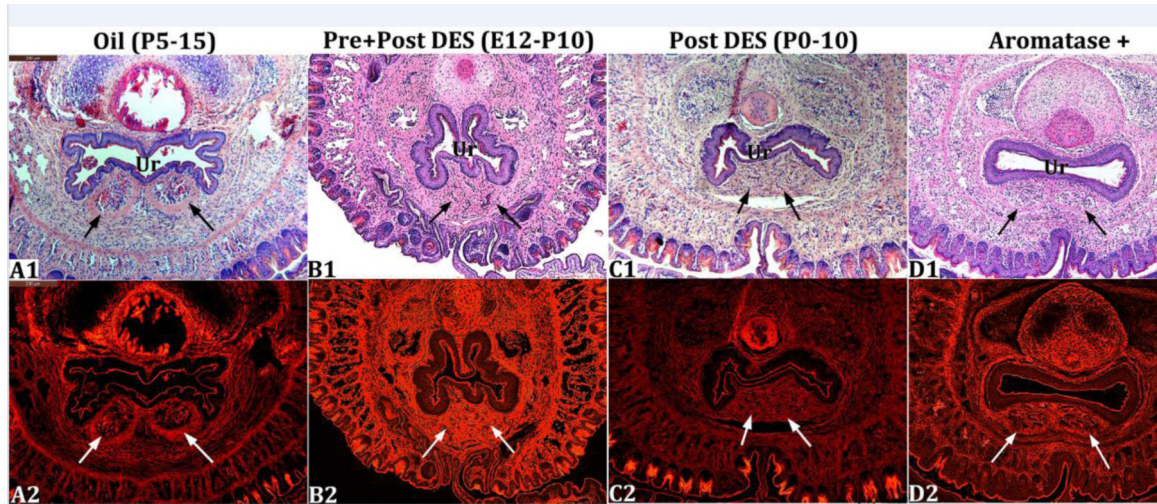
**Figure 1.**

Scanning electron micrographs of adult (60 day) mouse penises treated with oil vehicle and DES at the ages specified. (A-F) = end on views, (G-L) = lateral views, (M-R) = ventral views. Severe truncation of the MUMP (green arrowheads in I & J), malformation of the urethral meatus with abnormal clefting patterns in the MUMP ridge (C & D) and the ventral tether (purple arrowheads in I, J, O, & P) are seen in the P0-P10 and E12-P10 groups. Other treatment groups show less severe malformation or minimal departure from the oil treated specimens. IP = internal prepuce, MR = MUMP ridge, MRG = MUMP ridge groove, VC = ventral cleft in MUMP ridge.



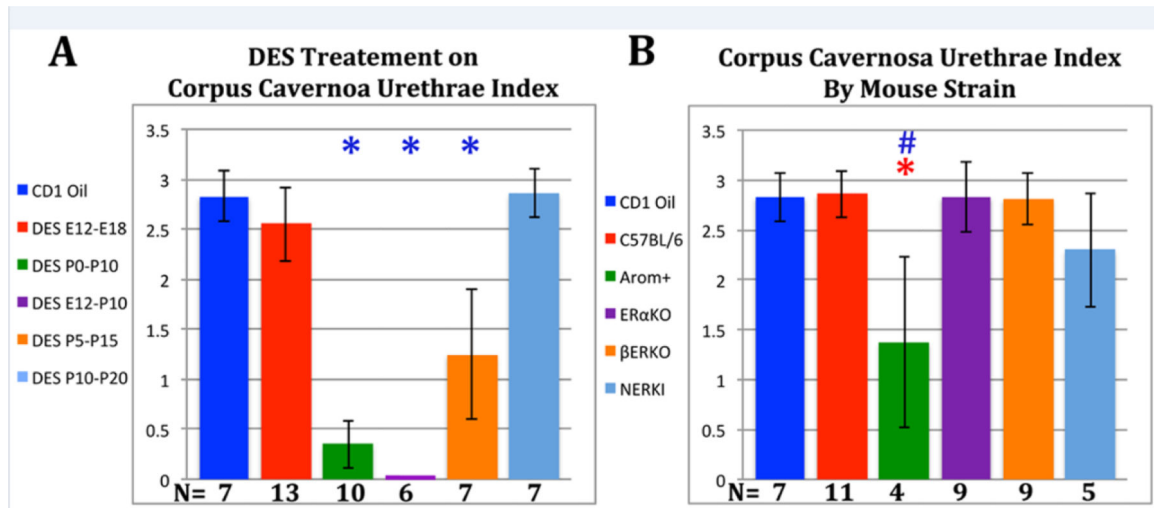


**Figure 2.** Histologic transverse sections exhibiting ventral tethering (arrows) of the ventral penile surface to the inner aspect of the prepuce. Such abnormal attachments are only seen in the treatment groups depicted. UR = urethra, B = bone, C = MUMP cartilage.



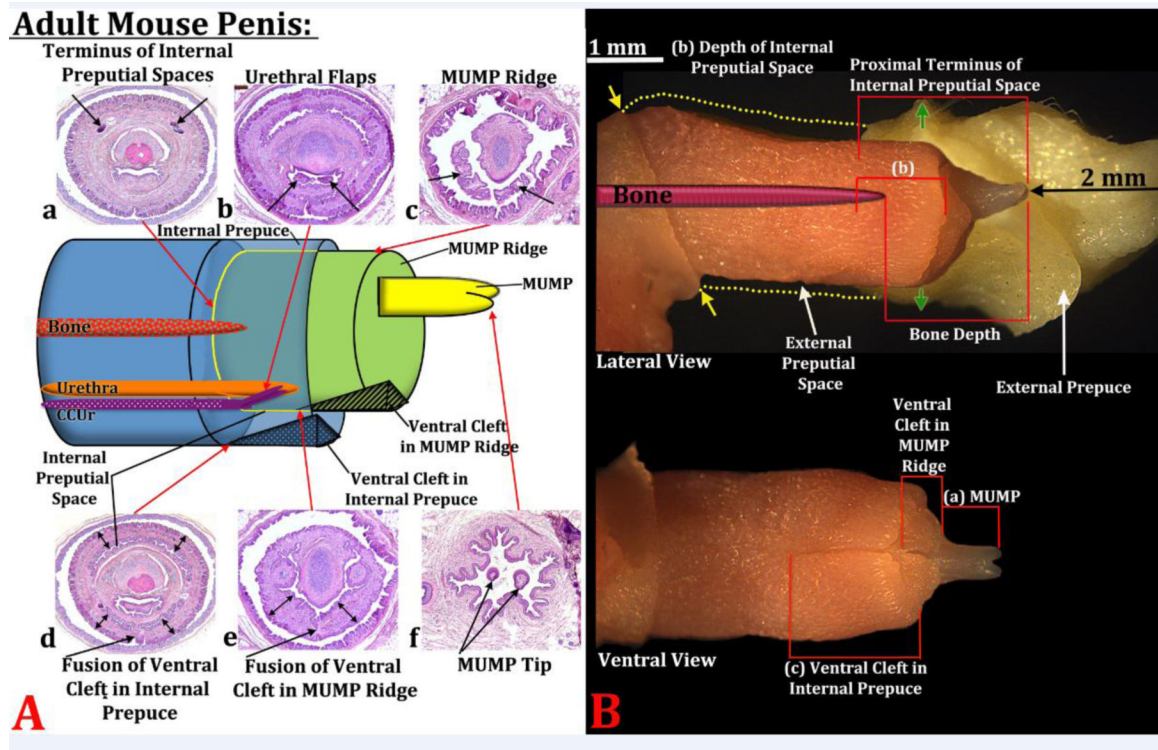
**Figure 3.**

Transverse histologic sections at the level of the corpora cavernosa urethrae (arrows). In A1 and A2 (oil-treated) the corpora cavernosa urethrae are well demarcated. In the DES E12-P10 (B1-B2) and DES P0-P10 (C1-C2) groups the corpora cavernosa urethrae are indistinct. In AROM+ mice (D1-D2) the corpora cavernosa urethrae are less well defined. Ur = urethra.



**Figure 4.**

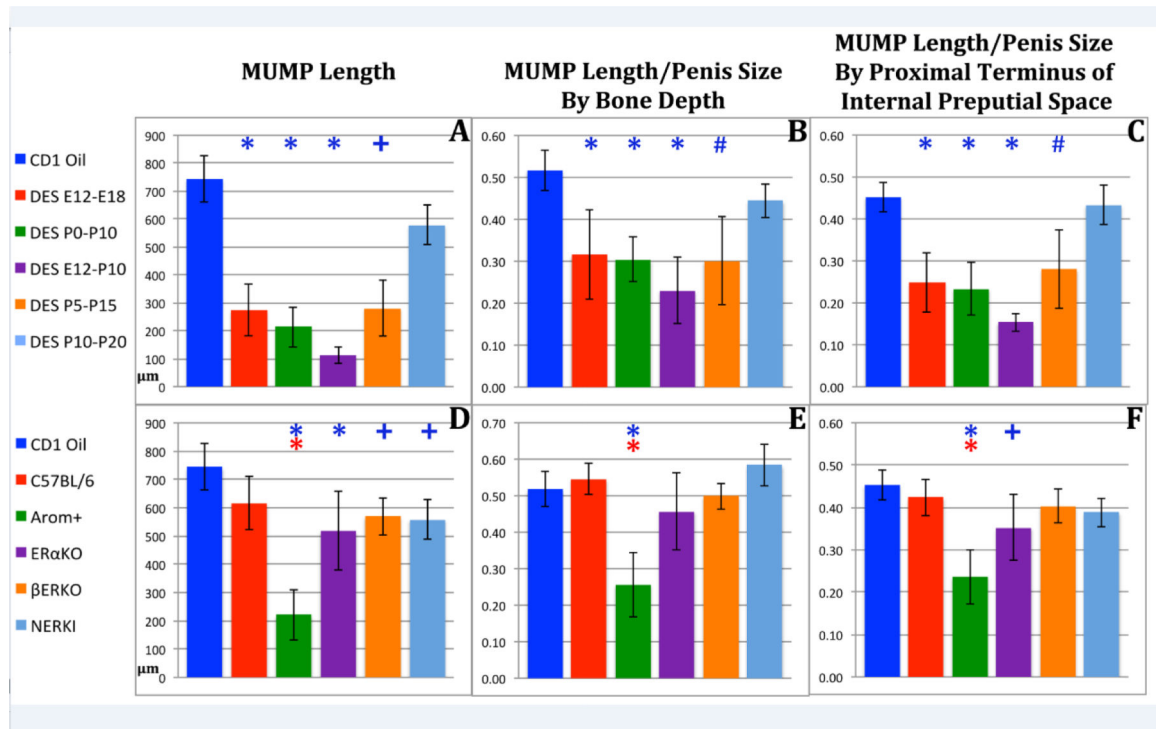
Corpora cavernosa urethrae index as described in the Materials and Methods. Note reduction in the corpora cavernosa urethrae index in the DES P0-P10, DES E12-P10, DES P5-P15 and AROM+ groups. Corpora cavernosa urethrae index was significantly altered relative to oil controls. When these symbols are depicted in blue, the data was normalized to values in CD-1 mice. When these symbols are depicted in red, the data was normalized to C57BL/6 mice. # =  $p < 0.001$  and \* =  $p < 0.0001$



**Figure 5.**

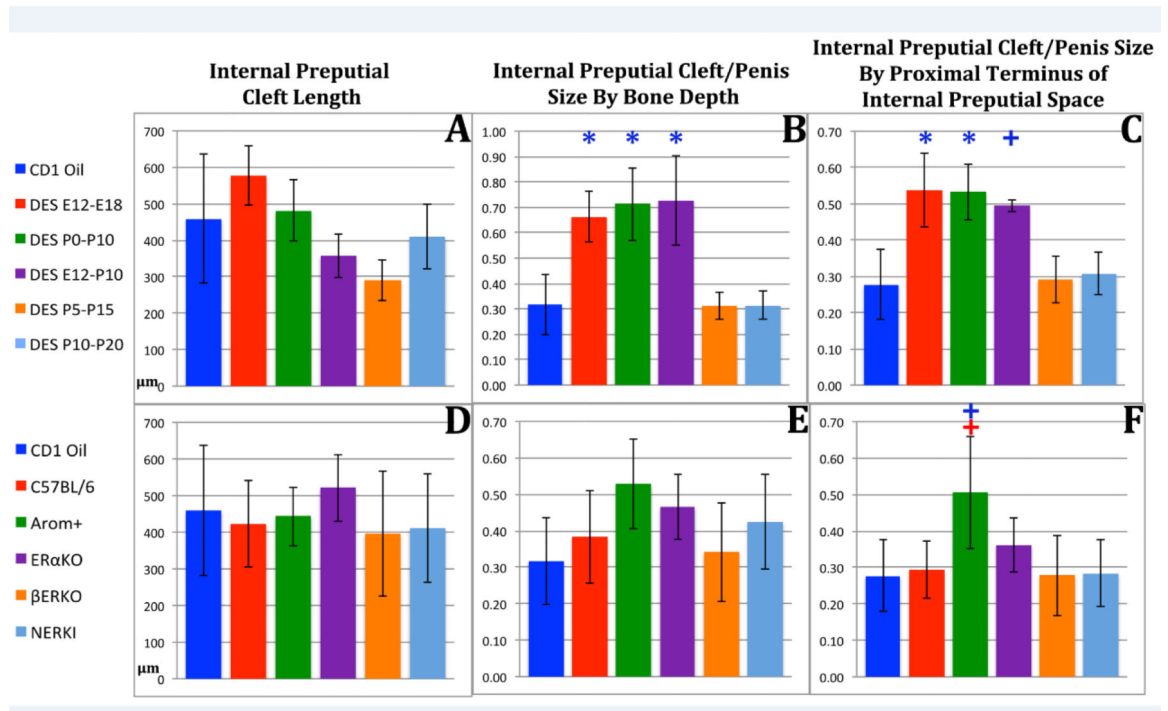
(A) Diagram indicating the positions of internal and external structures within the mouse penis with histological sections (a-f) at the position specified. In section (a) the arrows indicate the proximal terminus on the epithelium defining the internal preputial space, whose position is indicated by the red arrow meeting the yellow line. In section (b) the arrows indicate the urethral flaps. In section (c) the arrows denote the distal aspect of the MUMP ridge with the MUMP located dorsal to the MUMP ridge. Section (d) the arrow denotes the fusion of the ventral cleft in the internal prepuce and thus stromal confluence across the midline. The red arrow indicates the position of this event on the diagram. The double-headed arrows indicate the internal prepuce. Section (e) denotes the fusion of the ventral cleft in the MUMP ridge and thus stromal confluence across the midline. The red arrow indicates the position of this event on the diagram. The double-headed arrows indicate the MUMP ridge. Section (f) depicts the bifid tips of the MUMP. In all cases the red arrows indicate where sections (a-f) are located on the diagram. (B) Photographs of penises of 60-day untreated mice in lateral and ventral views showing how the morphometric measures were made. (a) MUMP length = distance from MUMP tip to where the MUMP joins the MUMP ridge. (b) Depth of the internal preputial space was measured from the most distal section containing the internal prepuce proximally to the last section containing epithelium of the internal preputial space. (c) Internal preputial cleft length was measured from the most distal section containing the internal prepuce proximally to the proximal end of the cleft in the internal prepuce. The last measure (not illustrated) is distal penile tip to urethral flaps, that is, distal most section containing the tip of the MUMP to the first section containing urethral flaps. In the lateral view “Proximal Terminus of Internal Preputial Space” and “Bone Depth” indicate the surrogates of penile length used to normalize data. The upper

image in (B) shows the external prepuce and the os penis (bone) superimposed. Yellow dotted lines indicated the full extent of the external prepuce, and the yellow arrows denote the reflection of the epithelium of the external prepuce onto the penile surface. Green arrows denote the point where the outer skin of the external prepuce becomes continuous with abdominal skin.



**Figure 6.**

Morphometric analysis of MUMP length in perinatally DES-treated and mutant mice expressed as absolute length (A & D) or normalized to surrogates of penile length (B, C, E, F). Significance symbols (\*, # and +) when depicted in blue indicate normalization to CD-1 mice and in red when normalized to C57BL/6 mice. + =  $p < 0.05$ , # =  $p < 0.001$  and \* =  $p < 0.0001$ .



**Figure 7.** Morphometric analysis of internal preputial cleft length in perinatally DES-treated and mutant mice expressed as absolute length (A & D) or normalized to surrogates of penile length (B, C, E, F). Significance symbols (\* and +) when depicted in blue indicate normalization to CD-1 mice and in red when normalized to C57BL/6 mice. + =  $p < 0.05$  and \* =  $p < 0.0001$ .

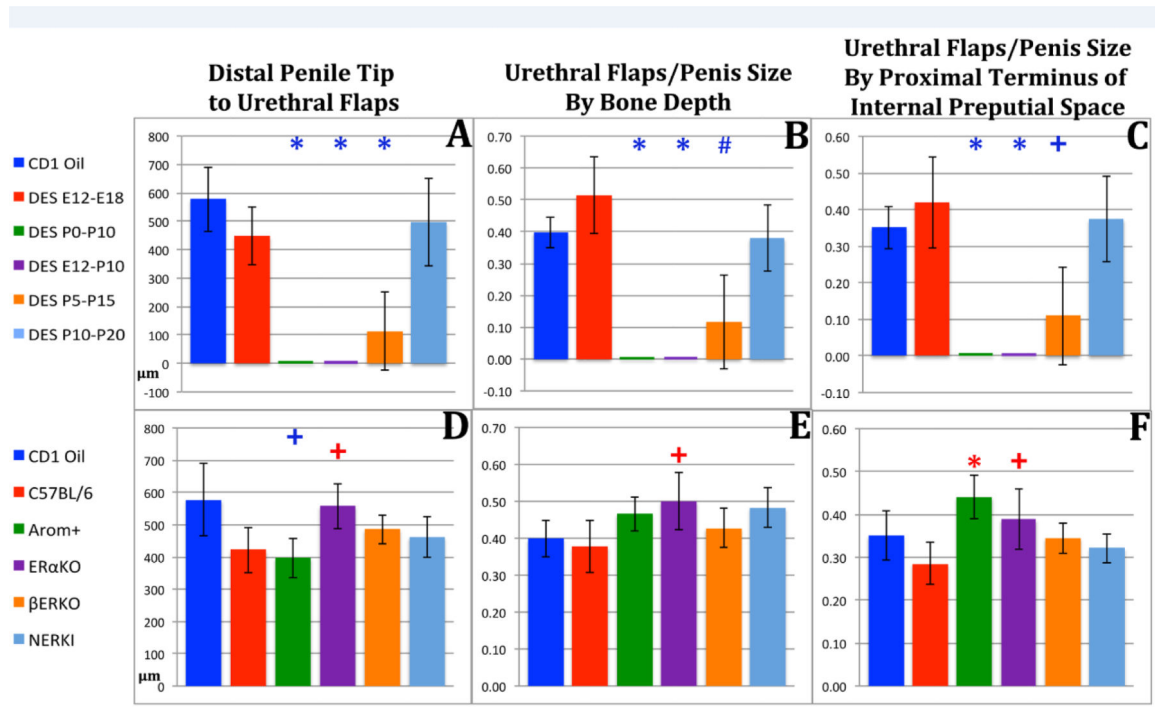


**Figure 8.**

Morphometric analysis of distal penile tip to urethral flap length in perinatally DES-treated and mutant mice expressed as absolute length (A & D) or normalized to surrogates of penile length (B, C, E, F). Significance symbols (\*, # and +) when depicted in blue indicate normalization to CD-1 mice and in red when normalized to C57BL/6 mice. + =  $p < 0.05$ , # =  $p < 0.001$  and \* =  $p < 0.0001$ .



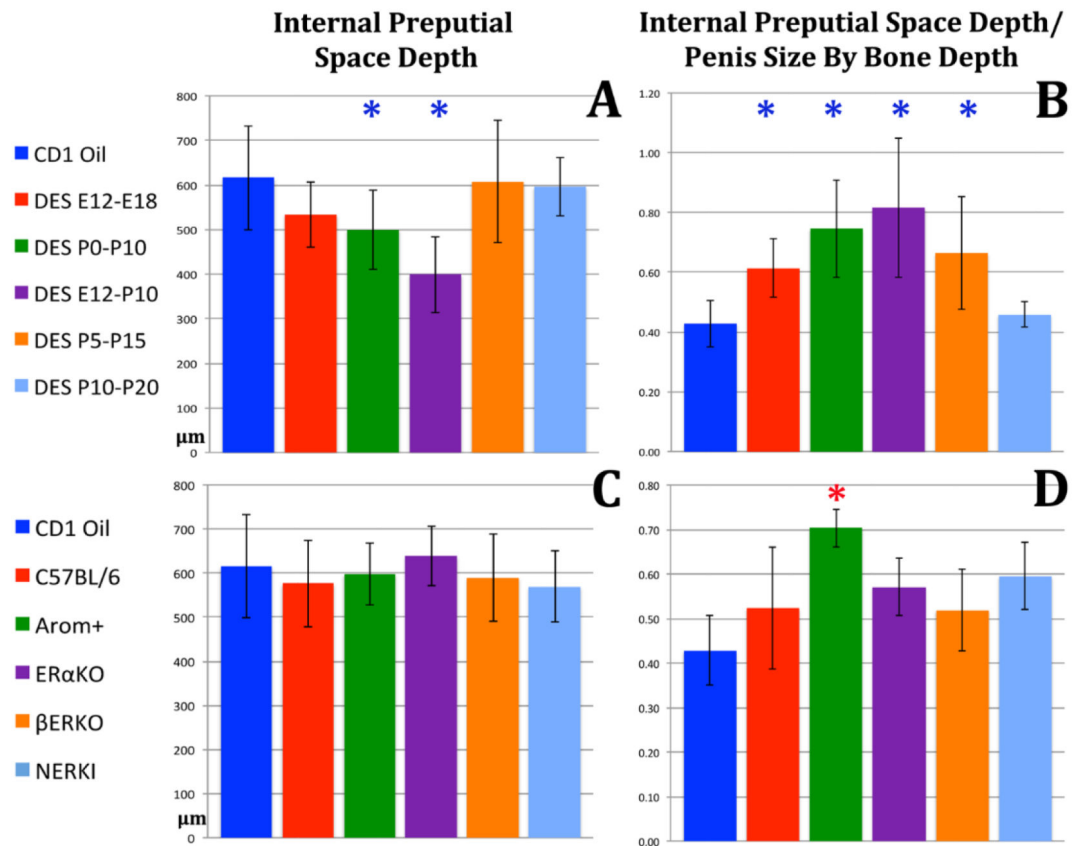


**Figure 9.** Morphometric analysis of internal preputial space depth in perinatally DES-treated and mutant mice expressed as absolute length (A & D) or normalized to surrogates of penile length (B, C, E, F). Significance symbol (\*) when depicted in blue indicate normalization to CD-1 mice and in red when normalized to C57BL/6 mice. \* =  $p < 0.0001$ .

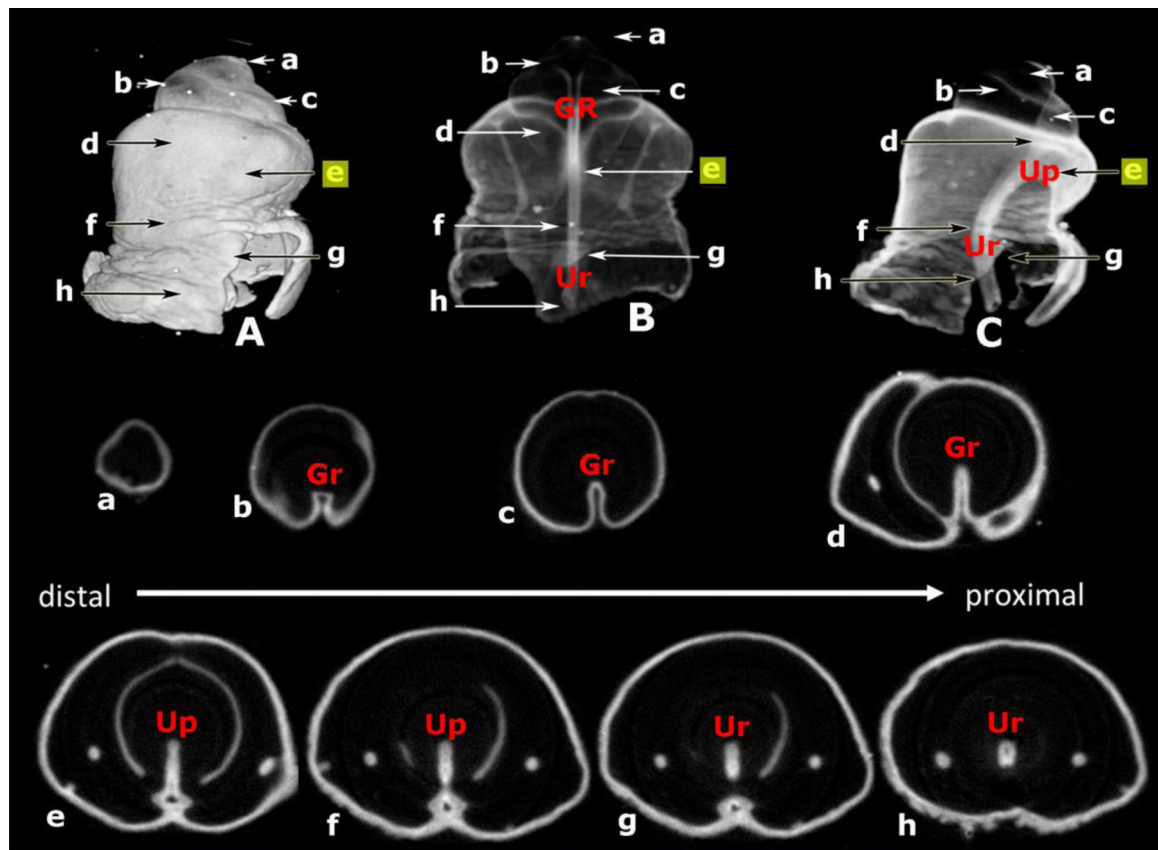


**Figure 10.**

Optical project tomography (OPT) images of the genital tubercle of a 16-day embryonic male mouse stained with anti-E-cadherin to reveal epithelium. (A) is a surface rendered lateral view. (B) is a semi-transparent dorsal-ventral view. (C) is a semi-transparent dorsal-ventral view. Note that the distal aspect of the genital tubercle is very faint in (B) and (C). OPT sections (a-h) organized in distal (a) to proximal order (h) indicate the morphology at the positions specified. Note the absence of the urethral plate (Up) in sections (a-d) where the ventral groove (Gr) is present. The urethral plate (Up) (with or without canalization) is seen in sections (e-h). Ur = urethra. Position of section (e) highlighted in yellow indicates the distal terminus of the urethral plate.

**Table 1**

Treatment Groups and Age of Analysis.

<b>Treatment Group</b>	<b>Treatment Period</b>
Prenatal DES	E12-E18 (N=10)
Postnatal DES	P0-P10 (N=12)
Prenatal + Postnatal DES	E12-P10 (N=6)
Postnatal DES	P5-P15 (N=7)
Postnatal DES	P10-P20 (N=7)
Oil	All of the above groups (N=39)

E= embryonic, P= postnatal

Author Manuscript

Author Manuscript

Author Manuscript

Author Manuscript